IAC-24-C2.6.9

Wear-Resistance Investigations on Ceramic Coatings for Lunar Dust Mitigation

Zachary Stein[a], Ashley Tirado-Pujols[b], Christopher Wohl[c], Valerie Wiesner[d] Seetha Raghavan[e*]

[a] *Department of Aerospace Engineering, Embry-Riddle Aeronautical University, Daytona Beach, Florida, 32114 United States, steinz@my.erau.edu*
[b] *Department of Aerospace Engineering, Embry-Riddle Aeronautical University, Daytona Beach, Florida, 32114 United States,* tiradopa@my.erau.edu
[c] *Advanced Materials and Processing Branch, National Aeronautics and Space Administration (NASA), Hampton, Virginia, 23693 United States, c.j.wohl@nasa.gov*
[d] *Advanced Materials and Processing Branch, NASA, Hampton, Virginia, 23693 United States, valerie.l.wiesner@nasa.gov*
[e] *Department of Aerospace Engineering, Embry-Riddle Aeronautical University, Daytona Beach, Florida, 32114 United States, seetha.raghavan@erau.edu*
* Corresponding Author

Abstract

Lunar dust has posed a major challenge to exploration efforts due to abrasion and impact. This work focuses on fundamental studies on ceramic coatings as candidates for enhanced resistance to impact and wear. As a first step, standard and modified approaches to the method of abrasion testing were explored for options to incorporate lunar regolith as wear media, the effects of which were presented for AL6061-T6 control samples. Following this, wear results for air plasma-sprayed (APS) alumina coatings were investigated due to their superior strength and surface hardness. In addition, APS 8 wt % yttria-stabilized zirconia (8YSZ) coatings were studied for their strength and martensitic transformation toughness. Measurements were made by assessing the mass loss, with a standard scale at various intervals. In addition, surface roughness was measured with a profilometer and features identified with a high-resolution microscope. The findings demonstrated that wear media has a distinct effect on the abrasion. The alumina coatings demonstrated improved wear over 8YSZ. However, the tailorability of 8YSZ makes it an attractive option to continue to modify as a wear-resistant coating to protect against lunar dust abrasion. The results of these measurements provide insight into the wear behavior of future directions in candidate ceramic coatings for the harsh lunar environment.

Keywords: Ceramic coatings, Abrasion testing, Wear

Acronyms/Abbreviations

Air Plasma Spray (APS)
Yttria-Stabilized Zirconia (YSZ)
Lunar Mare Simulant (LMS)
Lunar Highland Simulant (LHS)

1. Introduction

The foundation for a sustained presence on the Moon relies on designing material systems that are resilient to the harsh conditions on its surface. The resources that will be deployed on upcoming NASA's Artemis missions ranging from human landing and exploration systems to astronaut spacesuits need protection from exposure to lunar dust and micrometeorites, as well as temperature variations and cosmic radiation, to ensure operability.

Lunar dust, specifically, has the potential to impede any planned operation on the lunar surface. The technological issues related to lunar dust were first identified during the Apollo missions and include overheating, abrasion, and clogging of lunar surface equipment, as well as health problems for astronauts [1,2]. Among these various concerns, abrasion from lunar dust has been identified as an area of high importance for future exploration missions, because it affects any space system component that comes into contact with dust [1-5]. Especially, the abrasive nature of lunar dust is a result of the fine-grained, sharp and jagged edges they possess. This is due to the unique weathering conditions on the lunar surface, including continuous micrometeorite bombardment and lack of mechanical weathering and atmospheric passivation [4,5].

Various methods to mitigate the abrasion and erosion effects of lunar dust have been and are currently being researched [2-7]. Ceramic coatings, in particular, have the potential to reduce lunar dust adhesion while providing enhanced durability due to superior abrasive and/or erosive wear-resistant properties compared with traditional polymeric and metallic materials [6-9]. Design and manufacturing of these coatings have evolved over decades to achieve optimal performance for a range of industrial applications to improve wear and erosion resistance, corrosion protection and thermal insulation of the metallic surfaces [10-14]. Leveraging this mature coating technology offers the potential to fast-track the design of optimal ceramic coating systems that address lunar dust abrasion and provide long term durability. This work focused on the investigation of candidate coatings of alumina and yttria stabilized zirconia (YSZ) ceramics for the wear-resistance that they offer. Abrasion testing methods using different wear media were first assessed on bare 6061 aluminum alloy (Al6061-T6) substrates followed by similar tests on coated substrates.

1.1 Air plasma spray ceramic coatings

The method of coating deposition plays an important role on the resulting microstructure of the coating and consequently its wear resistance. Air plasma spray (APS) is an established technique that produces versatile engineering coating systems to protect underlying metallic materials against wear, friction, corrosion, high temperatures and other harsh environments [5]. Ceramics, such as alumina and YSZ, possess desirable properties, including high strength and hardness, and have been demonstrated to have excellent resistance to different types of wear [6, 7]. These coatings are often deposited via APS. However, these coatings are also known for thermally induced microcracks within splats and porosity that affect their mechanical properties.

APS coatings are typically deposited on metal substrates with or without a bond coat (BC). This metallic alloy interlayer promotes adhesion and oxidation resistance of the top coat (TC) ceramic to the substrate [14]. Since the mechanical interlocking of the first layer of splats with the bond coat surface has an impact on the durability of the coatings [14], sample configurations with and without a bond coat are considered in this work to capture any effects of BC on wear performance.

1.2 Abrasion testing methods and wear media

Abrasion testing is a critical step in selecting materials for use in the design of future lunar surface exploration architectures. The appropriate tests representative of the environment are key to the design of material systems that will demonstrate resilience in actual long-duration missions on the Moon. The process of designing the approach for testing materials under various scenarios of abrasion and impact related to lunar dust is evolving. Dust interactions occur when materials (substrates) representing space systems or vehicles either come into direct contact with lunar dust (a two-body problem) or when dust is trapped between two surfaces in relative motion (a three-body problem) [17,18].

Efforts were made to introduce lunar dust simulants as abrasives into a three-body test on various substrate materials ranging from soft polymers to metallic materials including Al6061-T6 and steel [17,18]. The results indicated that lunar dust simulants can be expected to produce a range of wear effects on various materials. The data indicated that lunar dust simulants have comparable abrasivity to silica on the softer substrates but the abrasivity varies on Al6061-T6 depending on the type of simulant used. It was determined that a combination of larger particle sizes and variation in mineralogy among simulants have an impact on the wear volume.

The findings demonstrated the need for innovative test methodologies that more accurately simulate the abrasive conditions of the lunar environment. Motivated by this need, the tests on Al6061-T6 presented in this paper use standard CS-17 wheels for a two-body test and introduce new regolith wheels made with lunar mare simulant-1 (LMS-1, Space Resource Technologies) with mean particle size > 60μm in a collaborative effort with Taber Industries. The tests follow ASTM D4060 standard for abrasion resistance of organic coatings [15].

1.3 Abrasion testing on ceramic coatings

Wear resistance of ceramic coatings, such as alumina and zirconia, has been significantly researched over decades [19, 20]. In general, the higher hardness of alumina over zirconia is such that under pure abrasive wear, where third body abrasive wear particles are present, alumina often outperforms zirconia. However, the higher toughness of zirconia over alumina reduces the spread of impact cracks and the microfracture of the surface, which generates erosive wear debris. In addition, the stabilization of zirconia with yttria enhances the strength and fracture toughness. In particular the fully stabilized 8 wt % yttria stabilized zirconia (8YSZ) is attractive for its resistance to thermal cycling [21]. The tailorability of YSZ is thus an attractive feature when considering optimizing a material system for lunar dust abrasion. The displacive tetragonal (t) to monoclinic (m) phase transformation can be used to enhance the strength and fracture toughness through careful microstructural control [22]. Additionally, microstructure and porosity are crucial parameters in wear resistance. It has been shown that coatings with more homogeneous and denser structures generally perform better in abrasion and erosion compared to poorly structured coatings. [23]. For example, directional freeze casting has been used to incorporate columnar pores into ceria-stabilized zirconia ceramics, thereby producing honeycomb-like structures. This structure circumvents the volume expansion that accompanies the martensitic transformation which causes mismatched stresses at grain boundaries in polycrystalline systems, leading to cracking and premature failure. The result can create either shape-memory or superelastic behavior under uniaxial compression [24]. In this work both alumina and YSZ coatings were tested under abrasion and their wear behavior compared.

2. Material and methods

2.1 Sample preparation

For the APS of the alumina and 8-YSZ coatings, a precursor powder is fed into a discharge plasma, where the particles melt and form small droplets which are accelerated towards the substrate. The droplets impact on the substrate surface, spread out and solidify to build up a lamellar structure resembling randomly stacked pancakes, often referred to as splats. The microstructure of plasma sprayed coatings, and thereby their mechanical properties is directly coupled to the deposition parameters. For the coated samples, Al6061-T6 substrates were grit blasted to increase surface roughness and provide mechanical interlocking for the plasma sprayed particles. APS was then used to deposit a bond coat with a composition of nickel, chromium, aluminum and yttrium (NiCrAlY) (Praxair, NI164-211). A summary of the sample material configurations is presented within Table 1.

Table 1. Coating material parameters

	Al6061-T6	Alumina w/o BC	Alumina	8-YSZ
BC (μm)	-	-	100	123.8 ± 45.9
TC (μm)	-	461.3 ± 21.9	581.4 ± 20.7	358.8 ± 45.9

2.2 Abrasion testing

Abrasion testing was conducted with a two-body QualTest GT-7012-T based on ASTM D4060 standard to ascertain wear performance. Abrasive wheels (CS-17 Calibrase wheels, Taber Industries) composed of a proprietary resilient binder and silicon carbide abrasive particles were used during the wear experiment. A custom abrasive wheel composition developed from LMS-1 simulant with proprietary resilient binder was introduced in this initial effort for comparative testing of the effects of abrasive in the abrasion test of the Al6061-T6 samples. The mass and layer thickness of each specimen was recorded with a weight balance (Analytical Balance ML204T/00) and a calibrated Eddy current coating thickness gauge instrument (Checkline DCN-3000FX), respectively, prior to performing the wear test.

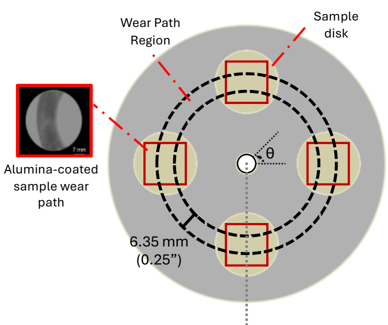

Fig. 1. Proportionally accurate schematic (top view) of four samples secured in a specimen holder with the circular path of the wheel and wear region marked and square region highlighting corresponding optical image of specimen.

All samples within Table 1 were tested up to 5,000 cycles, with each cycle being defined as a full disk rotation. The wheels were each loaded with 500 gram (g) weights to apply a constant normal force onto the surface of the coatings, allowing for a frictional abrasive action to occur. These abrasion tests were conducted on four one-inch-diameter samples of the Al6061-T6 control and 8YSZ samples and three one-inch-diameter alumina samples. Mass measurements of each sample were taken throughout the 5,000 cycles to determine the wear rate of the samples.

2.3 Wear characterization

Optical microscopy measurements were collected using a Keyence VHX-7000 at 200x magnification within the pristine and abraded regions of each sample. Profilometry data was collected using a Keyence VR-6000 at 40x magnification. Profilometry roughness measurements were calculated by taking a 10-line average across the length of the probed area and within three different locations within the probed area for both the pristine and abraded regions.

3. Theory and calculation

The wear behavior of the materials was assessed using the standard approach of tracking mass loss over cycles set forth in the ASTM D4060 standard.

3.1 Mass Loss

Measurements for wear are based on mass loss after abrasion:

$$\delta W = W_1 - W_2 \quad (1)$$

where δW is weight loss in milligrams (mg), W_1 corresponds to weight before abrasion in mg and W_2 is weight after abrasion in mg.

3.2 Wear Index

The wear index is a measure that indicates the rate of wear of a material [22]. The wear index (I) is calculated using Eq. 1, such that δW is the mass loss, and C_T is the total number of abrasion cycles recorded:

$$I = \frac{1000 * (\delta W)}{C_T} \quad (2)$$

It should be noted a material is more abrasion resistant when the wear index is lower. Within this study, the wear index is reported as the average wear rate for each sample type in mg per 1,000 cycles.

4. Results

4.1 Results on abrasion testing and wear media

The optical microscope measurements of the uncoated Al6061-T6 control can be found in Fig. 2. All optical measurements in Fig. 2 were collected with a 200x magnification.

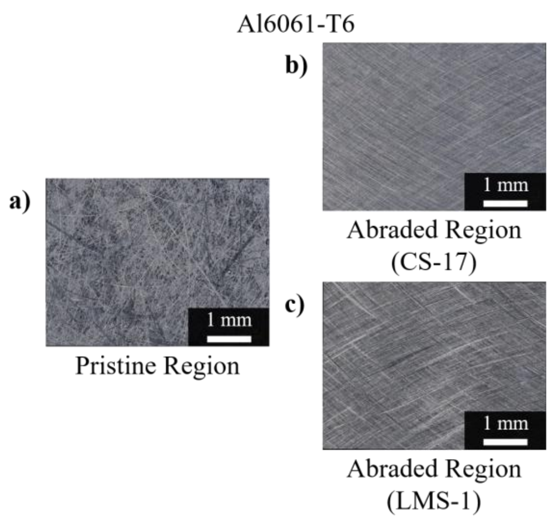

Fig. 2. Al6061-T6 control with (a) Pristine and (b) Abraded regions (CS-17) (c) Abraded region (LMS-1)

The wear path for the bare Al6061-T6 specimens serves as a baseline of how wearing occurred on the ceramic coatings within Figs. 2 – 4. It can be observed within Fig. 2(b) that the standard CS-17 wheels scratch the surface of material leaving a cross-hatched pattern as the wheels roll over the samples within the wear region. Overall, the scratches were relatively fine and appeared to be uniform across the specimen surface within the wear path. This is the result of the uniform grain size and hardness of the abrasive particles within the CS-17 wheel. The wear rate of the Al6061-T6 is determined by calculating the wear index given in Eq. 2, the results of which are reported in Table 2. Also reported in Table 2 are the average surface roughness measurements for both the abraded and pristine regions, with the latter roughness values presented in the table in parenthesises. The summary of the wear results is presented in Table 2 along with the surface roughness values measured through the average roughness using profilometry.

Table 2 shows that applying the CS-17 wheel results in the specimens having a wear index approximately 0.35 mg over 1000 cycles lower than that caused by contact with the LMS-1 wheel. Additionally, the average surface roughness of the sample within the abraded region was approximately 35% lower for the Al6061-T6 specimen using the standard wheels versus LMS-1-based wheels. The average surface roughness of the pristine regions was roughly 50% higher than the abraded regions and are reported within Table 2.

Table 2. Overall summary of results of Al606-T6 wear

	Al6061-T6 (Std wheel)	Al6061-T6 (LMS-1 wheel)
Wear index (mg/1000 cycles)	3.29	3.64
Average surface roughness (Ra) (μm) Abraded (Pristine)	0.68 ± 0.02 (1.28 ± 0.04)	0.97 ± 0.03 (1.83 ± 0.07)

4.2 Results on abrasion testing of ceramic coatings

Optical microscope measurements, taken with a 200x magnification, of the APS alumina coating without and with the BC are shown in Fig. 3 and Fig. 4, respectively, and the APS 8YSZ coating is displayed in Fig. 5.

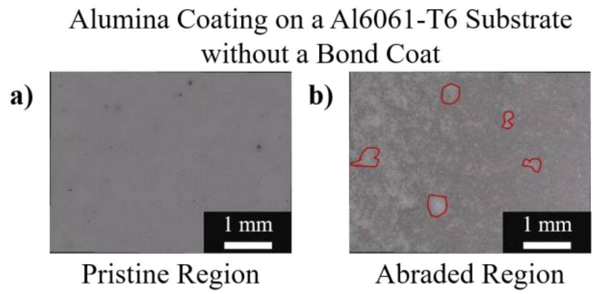

Fig. 3. (a) APS Alumina coating without BC with (b) pristine and (c) abraded regions with clusters of remaining alumina coating outlined in red

There are no discernible differences on the surface of the alumina coatings when comparing to those deposited with and without the inclusion of a bond coat onto the Al6061-T6 substrate, refer to Fig. 3(a), as ascertained in a previous study [16]. There are, however, discernible differences when comparing the wear path characteristics of the APS alumina coating without a bond coat, Fig. 2(b), to the APS alumina coating with a bond coat, Fig 3(b). Clusters of remaining alumina coating are outlined in red in Fig. 4. These speckled clusters, which is likely alumina, appear to be smaller and grainy in the alumina coating without a bond coat, Fig. 2(b), when compared to the higher concentrations within the alumina coating with a bond coat, Fig. 3(b). Meanwhile, the alumina coating with the bond coat appears to have larger globular connected regions of high alumina coating concentrations. This is likely an effect of the underlying microstructure layer underneath the alumina, its roughness and the adhesion strength of that underlying layer. The effects of the underlying microstructure layer as well as the surface composition within the pristine and wear path are planned to be further investigated with electron microscopy.

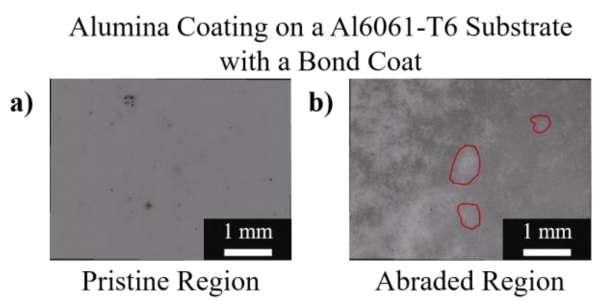

Fig. 4. APS alumina coating with BC with (a) pristine and (b) abraded regions with clusters of remaining alumina coating outlined in red

In both cases, the Al6061-T6 substrate was grit-blasted before applying the next layer. This grit-blasting roughens the surface of the sample and promotes higher adhesion strength. The alumina was then deposited straight onto this grit-blasted Al6061-T6 substrate in the case without a BC. This deposition, during sample manufacturing, likely results in the interface between the alumina and the substrate having a wavy-like characteristic. Then, as the alumina is abraded away, this roughened interface is slowly exposed, leaving small pockets of alumina coating dispersed across the surface. Electron microscopy is planned to be conducted to further investigate this interfacing layer.

For the alumina coating with BC, the BC would act as the interface between the metallic substrate with the ceramic coating, increasing the adhesion strength of the alumina to the material system. It is also possible this increased adhesion with the inclusion of the bond coat limited potential micro-interfacial spallation during abrasion testing. However, additional investigations are necessary to further elucidate the effects of BC on the abrasion wear path and differences in surface roughness.

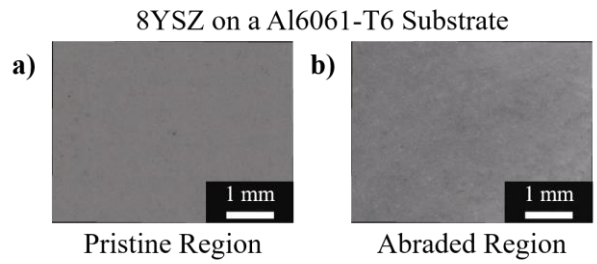

Fig. 5. APS 8YSZ coating with (a) pristine and (b) abraded regions

Meanwhile, it can be observed in the 8YSZ coating, shown in Fig. 5(b), that the wear path is more uniformly abraded as compared to the alumina coating samples. This is likely due to 8YSZ being softer than alumina [25]. This results in the 8YSZ being more prone to abrasion than alumina. This higher abrasion and wear rate is indicated by the higher wear index presented in Table 3. Table 3 also includes surface roughness measurements taken from the average roughness values.

When comparing Table 2 with Table 3, the Al6061-T6 control samples possessed the lowest wear index. With the coated samples, the wear index is roughly the same for both the alumina without a BC as with the BC. Only a slight increase of 0.2 mg per 1000 cycles in the overall wear rate is observed with the addition of the BC. Finally, the 8YSZ has a wear rate of nearly double that of the alumina coating samples. This indicates the 8YSZ coating abrades roughly twice as much as the alumina coating samples.

The average surface roughness values were determined for both before and after the abrasive wear tests were conducted. In all cases, the average surface roughness decreased, which is a result of the abrasive wheels abrading away the unevenness of the surface.

When comparing the average pristine surface roughness, it was observed that the 8YSZ specimens had the highest roughness, followed by the alumina coating with BC, the alumina coating without BC, and finally, the Al6061-T6 control samples.

The data suggests a relationship between the average surface roughness prior to wear testing and the wear index. This is likely due to the reduced number of contact points between the wheels and rougher coating surfaces, resulting in an increasing concentration of the applied abrasive forces. This is in comparison to a smoother surface, where there is an increased number of contact points between the wheels and surface, when considering minimal auxiliary loading. This smoother surface results in more even wearing on the coating. However, more work needs to be done to determine the relationship between surface roughness and wear rate.

Table 3. Overall summary of results of APS coating wear

	Alumina w/o BC	Alumina w/ BC	8YSZ w/BC
Wear index (mg / 1000 cycles)	5.19	5.39	9.20
Average surface roughness (R_a) (µm) Abraded (Pristine)	2.79 ± 0.15 (3.70 ± 0.27)	4.64 ± 0.17 (5.69 ± 0.27)	4.11 ± 0.33 (8.72 ± 0.27

5. Discussion

5.1 Abrasion testing and wear media

The results of wear from the standard CS-17 and LMS-1 wheels demonstrate a slightly higher wear index resulting from testing with the LMS-1 wheels. This indicates that the wear media in the test process has an influence on the overall wear index and consequently abrasion performance of a material. This assessment is in lines with previous efforts using three-body tests that have lunar dust introduced as abrasive media [17,18]. This awareness of the effects of lunar dust simulant in materials testing is critical to achieve results that are more representative of the environment in which the materials will be used. The various locations on the lunar surface have different mineralogy compositions and particle sizes. An abundance of harder minerals and larger particle sizes can exacerbate the effect of long-term wear on a material system. The ability to incorporate additional simulant compositions in abrasion testing will allow for more effective design of material systems for the lunar missions. This initial introduction of regolith wheels paves a way to assess different wear media using a two-body approach. These results set the stage for advancing abrasion testing methods. Future tests will incorporate various wear media in abrasion testing of ceramic coatings.

5.2 Abrasion testing of ceramic coatings

The optical micrographs of the alumina coatings shown in Fig. 3 and 4 demonstrate differences with respect to wear path and surface characteristics when compared to that of the 8YSZ coating. The speckled clusters shown in Fig. 3 for the alumina coating could possibly be due to increased microcracking of the high hardness alumina. This is likely due to higher coating-grit contacting the pristine sample with lower surface roughness of alumina coating compared to 8YSZ. The alumina with BC demonstrates less of this effect, since the BC contributes to some ductility as an interface layer. For the 8YSZ, the marked increase in as-sprayed surface roughness has the opposing effect where lower coating-grit contact results in a more uniform wear surface.

In general, Table 3 indicates that the wear index is lower for alumina than 8YSZ suggesting that alumina possesses more wear resistance. This is expected due to the elevated hardness of alumina in comparison to 8YSZ. However, the tailorability and versatility of 8YSZ makes it an attractive option to continue pursuing as protective coatings for varied lunar applications, especially when considering extreme thermal variations that the harsh lunar environment poses. These thermal variations would likely be introduced through cyclical thermal shocks to materials as operation temperatures vary by over 300 K between daytime and nighttime temperature cycling [26]. The results indicate a need to compensate for the lower wear resistance. This can be explored by modifying the 8YSZ with additives including hard materials, such as carbides or nitrides.

5. Conclusions

This study investigated the wear behavior of ceramic coatings and utility of using lunar dust simulant as an abrasive media compared to more standard compositions. The first step was to address the wear media effect on abrasion testing. By introducing a unique approach of using regolith wheels in the abrasion test, the wear media was observed to impart a different wear response from the material compared to a standard abrasive. Further tests using various regolith simulants of different compositions and particle sizes will establish quantitative measures of the wear media effect. Additionally, further evaluation using characterization methods, such as electron microscopy, will provide a deeper understanding of the wear mechanisms and wear path characteristics of regolith simulants on various material systems relevant to lunar applications.

In the evaluation of APS alumina and 8YSZ, it was seen that the higher hardness of alumina translated to better wear performance. However, the toughness offered by 8YSZ and its tailorability through varied material processing and the inclusion of additives to strengthen its material properties make 8YSZ an attractive option to consider for an optimal protective coating against the harsh lunar environment.

Acknowledgements

This material is based upon work supported by the National Aeronautics and Space Administration under Grant No. 80NSSC21M0309 issued through the NASA Office of STEM Engagement (MSTAR) and from NASA Langley Research Center Innovation Fund and Space Technology Mission Directorate Game Changing Development Program.

The authors would like to acknowledge and thank Alan Janecke and Taber Industries for their support in manufacturing the regolith wheels used within this study.

References

[1] Gaier, J. R. (2007). The effects of lunar dust on EVA systems during the Apollo missions (No. NASA/TM-2005-213610/REV1).

[2] Kobrick, R. L., Klaus, D. M., & Street Jr, K. W. (2011). Defining an abrasion index for lunar surface systems as a function of dust interaction modes and variable concentration zones. Planetary and Space Science, 59(14), 1749-1757.

[3] Stubbs, T. J., Vondrak, R. R., & Farrell, W. M. (2005, October). Impact of electrically-charged dust on lunar exploration. In Space Resources Roundtable VII: LEAG Conference on Lunar Exploration (Vol. 1287, p. 85).

[4] Mishra, S. K., Prasad, K. D., Nath, P., Agarwal, D., Kumar, S. S., & Bhardwaj, A. (2022). Effect of lunar landing on its surface, surrounding environment and hardware: A numerical perspective. Planetary and Space Science, 211, 105398.

[5] Kruzelecky, R., Wong, B., Aissa, B., Haddad, E., Jamroz, W., Cloutis, E., et al. (2010). Moon Dust lunar dust simulation and mitigation. In 40th International Conference on Environmental Systems (p. 6023).

[6] Chinnusamy, S., Ramasamy, V., Venkatajalapathy, S., Kaliyannan, G.V., Palaniappan, S.K. (2019). Experimental investigation on the effect of ceramic coating on the wear resistance of Al 6061 substrate. Journal of Materials Research and Technology: 8(6): 6125-6133.

[7] Chelladurai, S. J. S., Kumar, S. S., Venugopal, N., Ray, A. P., Manjunath, T. C., & Gnanasekaran, S. (2021). A review on mechanical properties and wear behaviour of aluminium based metal matrix composites. Materials Today: Proceedings, 37, 908-916.

[8] Latorre-Suarez, P., Gucwa, K., Swaby, O., Bansberg, L., Fouliard, Q., and Raghavan, S. (2022). Investigating the Durability of Aluminum Oxide Coatings for Lunar Dust Mitigation. International Astronautical Congress 2022.

[9] Latorre, P. C., Fouliard, Q., & Raghavan, S. (2023). Characterizing Air Plasma Sprayed Aluminum Oxide Coatings for the Protection of Lunar Structures. In AIAA SCITECH 2023 Forum (p. 1517).

[10] Wiesner, V., Wohl, C., King, G., Gordon, K., Das, L., & Hernandez, J. (2023). Protective Coatings for Lunar Dust Tolerance, NASA TM 20230003195.

[11] Wang, X., Wang, W., Shao, H., Chao, S., Zhang, H., Tang, C., & Lu, Y. (2022). Lunar Dust-Mitigation Behavior of Aluminum Surfaces with Multiscale Roughness Prepared by a Composite Etching Method. ACS Applied Materials & Interfaces, 14(29), 34020-34028.

[12] Bowling, L., Horvath, B., & Wohl, C. (2021). Integration of advanced structures and materials technologies for a robust lunar habitat. In 2021 IEEE Aerospace Conference (50100), 1-13. IEEE

[13] Margiotta, D.V., Peters, W.C, Straka, S.A., Rodriguez, M., McKittrick, K.R., & Jones, C.B. (2010). The lotus coating for space exploration: a dust mitigation tool, Society of Photo-optical Instrumentation Engineers (SPIE) Conference Series, 7794.

[14] Gildersleeve, V V, E. J., Viswanathan, V., Lance, M. J., Haynes, J. A., Pint, B. A., & Sampath, S. (2019) . Role of bond coat processing methods on the durability of plasma sprayed thermal barrier systems, Surface and Coatings Technology, 375, 782-792.

[15] ASTM D4060-19, “Test Method for Abrasion Resistance of Organic Coatings by the Taber Abraser,” ASTM International, West Conshohocken, PA, 2019.

[16] Latorre-Suarez, P. C, Fouliard, Q., Wohl, C., Wiesner, V., & Raghavan, S. (2023). Measuring Wear and Abrasive Resistance of Air Plasma Sprayed Aluminum Oxide Coatings for Lunar Exploration. International Astronautical Congress, Baku, 2023.

[17] Kobrick, R. L., Klaus, D. M., & Street, K. W. (2019). Developing Abrasion Test Standards for Evaluating Lunar Construction Materials SAE International Journal of Aerospace 4(1).

[18] Kobrick R. L. (2010). Characterization and measurement standardization of lunar dust abrasion for spacecraft design and operations. University of Colorado at Boulder.

[19] Westergård, R., Axén, N., Wiklund, U., & Hogmark, S. (2000). An evaluation of plasma sprayed ceramic coatings by erosion, abrasion and bend testing. Wear, 246, 12–19

[20] Hannink, R. H. J., Kelly, P. M., & Muddle, B. C. (2000). Transformation Toughening in Zirconia-Containing Ceramics. Journal of the American Ceramic Society, 83

[21] Song, X., Zhang, J., Liu, Z., Jiang, C., Lin, C., & Zeng, Y. (2019). Thermal shock resistance of YSZ, YSZ-Al2O3 and YSZ-Al2O3/YSZ coatings. Vacuum, 162, 150-155.

[22] Kelly, P. M., & Rose, L. F. (2002). The martensitic transformation in ceramics—its role in transformation toughening. Progress in Materials Science, 47(5), 463-557.

[23] Quinn, L.K., Esteves, R., Latorre-Suarez, P. C., Rossman, G. R., Raghavan, S., & Faber, K.T. (2024). Shape memory and superelasticity in polycrystalline ceria-stabilized zirconia honeycombs Acta Materialia, 281, 120340

[24] Rahman, M.S.U. & Jayahari, L. (2018). Study of mechanical properties and wear behaviour of aluminium 6061 matrix composites reinforced with steel machining chips. Material Today Processing 5(9) 20117-20123.

[25] Singh, B. K., Ghosh, K., Roy, S. S., Mondal, B., & Mandal, N. (2018). Correlation between microstructure and mechanical properties of YSZ/Al2O3 ceramics and its effect on high speed machining of steel. Transactions of the Indian Ceramic Society, 77(4), 219-225.

[26] Williams, J. P., Paige, D. A., Greenhagen, B. T., & Sefton-Nash, E. (2017). The global surface temperatures of the Moon as measured by the Diviner Lunar Radiometer Experiment. Icarus, 283, 300-325.